VOL. 10, NO 20, NOVEMBER, 2015 ISSN 1819-6608
ARPN Journal of Engineering and Applied Sciences

www.arpnjournals.com

AREA CONTRACTION EFFECT ON SHOCK TUBE PERFORMANCE, NUMERICAL AND EXPERIMENTAL STUDY

A. M. Mohsen, M. Z. Yusoff and A. Al-Falahi
Centre for Fluid Dynamics (CFD), College of Engineering, Universiti Tenaga Nasional, Jalan Ikram-Uniten, Kajang, Selangor, Darul Ehsan, Malaysia
E-Mail: zamri@uniten.edu.my

ABSTRACT

The paper presents numerical and experimental study on the effect of area contraction in shock tube facility. The shock tube is the main component of short duration test facility at The Universiti Tenaga Nasional (UNITEN), Malaysia. In the shock tube, a small area contraction in form of a removable bush was facilitated adjacent to the diaphragm section. The flow process was simulated using a two-dimensional time-accurate Navier-Stokes solver. The solver uses second order accurate cell-vertex finite volume spatial discretization and fourth orders accurate Runge-Kutta temporal integration. In this study, the solver was programmed based on the dimensions and configuration of UNITEN's shock tube facility. The numerical results were validated with experimental data from the ground based test facility. Numerical pressure histories were found to be in accordance with the experimental data. For further investigations, simulations were conducted for different operating conditions. The results showed that shock tube performance in term of producing shock wave and steady gas flow is highly influenced by area contraction in the diaphragm section. The shock wave strength and speed decreased by 18% and 8% respectively.

Keywords: shock tube, area contraction, shockwave.

1. INTRODUCTION

Shock wave is a phenomenon of sudden change in pressure between narrow regions within a medium. To investigate such phenomenon, many studies have been reported. High speed flow test facilities have been developed and used in these investigations. Such facilities are known as shock tube, shock tunnel, and gun tunnel. Shock tube is one of the common methods of generating shock wave. This is done by rushing gas at high pressure into another at lower pressure by rupturing a thin diaphragm (Wintenberger *et al.*, 2002). The diaphragm separates the high pressure gas section from the one at lower pressure in the shock tube. The section which contains the high pressure gas is known as the driver section, while the lower pressure gas section is known as the driven section.

Short duration high speed flow test facilities have been very important in developing and testing of high-performance supersonic airplanes, as well as the hypersonic atmospheric re-entry of space vehicle. This requires deep understanding of the flow conditions that encountered by such vehicles during their actual flight. Such flow conditions can be explained as high temperatures, chemically reacting boundary layers, and shock layers. Accordingly, thorough experimental analysis in ground test facilities is important to simulate such conditions and apply comprehensive investigations (Briassulis *et al*., 1996; Satheesh *et al*., 2007). However, and due to extreme flow conditions and severe time constraint involved, it is quite difficult to fully examine all aspects of flow in ground based test facilities. Hence, numerical studies have become very important to provide a quantitative description on flow field conditions of such facilities (Wilson *et al*., 1993; Goozee *et al*., 2006]. For example, transient flow in shock tunnel facility has been investigated numerically by (Chue *et al*., 1998). Moreover, a numerical study using a finite volume based code was performed by (Jacob *et al*. 1991). In their study, the shock reflection process was simulated in an axi-symmetric shock tube and a high Mach number nozzle, using a perfect gas with no boundary layers applied on the shock tube walls.

Further studies have been reported on high speed flow in short duration test facilities. However, far too little attention has been paid to investigate the effect geometrical parameters on such facilities performance. In many short duration high speed flow test facilities, a small area contraction is used in the diaphragm section to facilitate diaphragm rupturing process. In the present work a numerical study and experimental measurements have been performed to investigate the effect of this contraction on shock wave strength, shock Mach number, and velocity profiles in a shock tube. The shock tube is an important component of a short duration high speed fluid flow test facility available at The Universiti Tenaga Nasional. The numerical investigations were performed with and without the presence of contraction. Three different diaphragm pressure ratios (P4/P1) of 10, 15 and 20 are used, and the results compared to selected set of experimental measurements. The instantaneous static pressure variations were stored at two different locations, using high sensitivity pressure sensors. This is to record and analyse

the shock wave strength, wave speed and peak pressure in the shock tube.

2. NUMERICAL PROCEDURE

A. Two-Dimensional CFD solver

A two dimensional time accurate Navier-Stokes solver was programmed based on the dimensions and configuration of the test facility. The solver has been recently developed in Universiti Tenaga Nasional (UNITEN) (Al-Falahi *et al*., 2008a). It uses second order accurate cell-vertex finite volume spatial discretization and forth orders accurate Runge-Kutta temporal integration, and can only simulate the flow process in the facility for similar driver/driven gases (e.g. air-air as working fluids). Only solid boundary condition is considered in the current work since the flow is confined within the tube. The no-slip boundary condition is imposed for the momentum equations and the adiabatic condition is assumed for the energy equation calculations. At present, the solver only able to handle the H-type mesh for the numerical simulations. The current program was developed and validated against exact solution (the Sod's tube problem) and experimental measurements in an earlier work by Al-Falahi *et al*. (Al-Falahi *et al*., 2008b). Only brief description of the solver is described in this paper interested readers can refer to References (Al-Falahi *et al*., 2008b; Al-Falahi *et al*., 2008c) for more details.

B. Mesh system

In the actual shock tube, a bush was inserted in the diaphragm section adjacent to the primary diaphragm to facilitate its rapture process; details of the bush are discussed in the following section. Since the solver can only handle H-type mesh, abrupt changes in geometry such as the exact shape of the bush, cannot be modelled. In order to represent the bush in the solver, an artificial wedge was included as shown in Figure-1. A variety of wedge angles has been simulated and the angle of 5° yields the best agreement against the experimental results (Al-Falahi *et al*., 2008c). Sample of mesh generation at the bush section for real dimensions of the facility is shown in Figure-2.

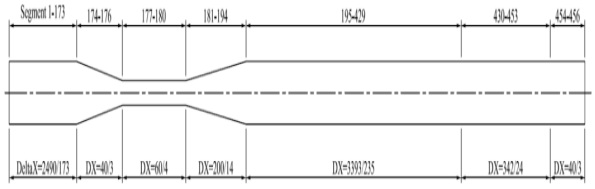

Figure-1. Mesh spacing allocated for each section.

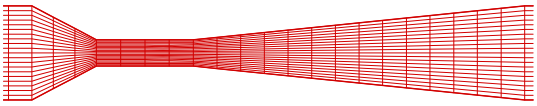

Figure-2. Mesh generation at the contraction section.

3. EXPERIMENTAL PROCEDURE

The diaphragm section of the shock tube consists of two flanges. It is designed to connect the driver section to the driven section and hold a thin aluminum diaphragm. The inner diameter of both driver and driven sections is 50 mm. The diaphragm section is shown in Figure-3.

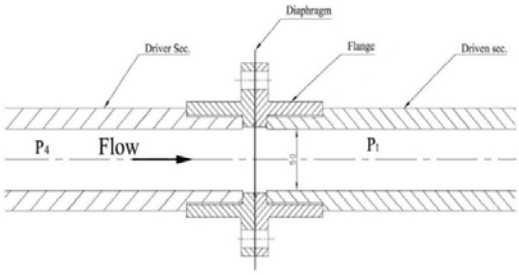

Figure-3. The diaphragm section (Mohsen *et al.* 2012).

When the facility was developed, a small area contraction in form of a removable bush was positioned in the driven section adjacent to the diaphragm. This is to facilitate diaphragm rupturing process and avoid any shear caused by the internal sharp edge of the driven section flange as shown in Figure-4.

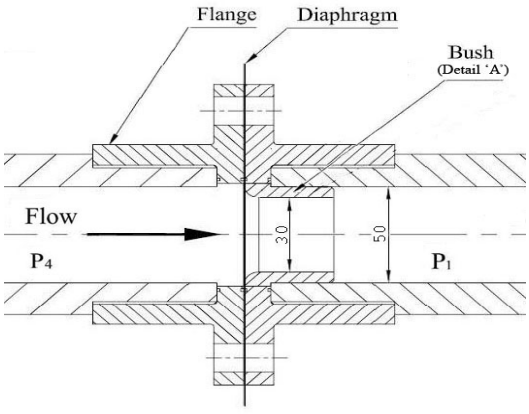

Figure-4. Bush location adjacent to the diaphragm (Mohsen *et al*. 2012).

However, in the present work, the measurements were performed with and without area contraction to study its effects on the facility performance. In contrast, the internal sharp edge of the driven section flange is rounded

with radius of 8 mm (see Figure-5) to facilitate diaphragm rupturing process when the facility is operated without the presence of the bush.

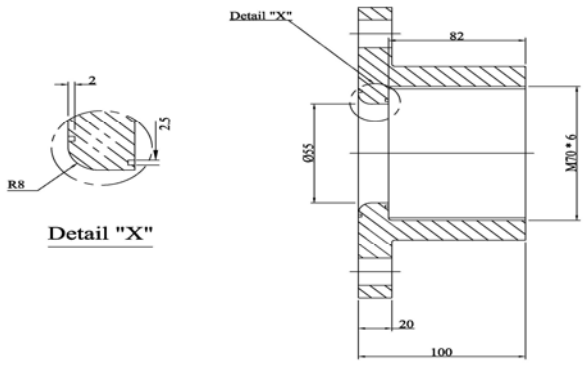

Figure-5. The driven section flange (Mohsen *et al*. 2012).

The experimental measurements were conducted at different operating conditions. To investigate the parameters of interest, first set of measurements were done with area contraction in the facility. In these experiments, a gas combination of Air-Air as the driver/driven gases with three different driver pressures, P4 = 1000, 1500, and 2000 KPa were used to obtain the sudden burst in the diaphragm and generate shock wave. The driven section pressure P1 is 100 KPa for all cases. The same set of experiments was repeated without area contraction in the facility (without the presence of the bush). The obtained data were compared to the numerical results.

In order to record the instantaneous pressure history in the driven section, two piezoelectric pressure transducers have been mounted at the end of the driven section. The position of the first pressure transducer is termed as station 1 and the second position is termed as station 2 (see Figure-6).

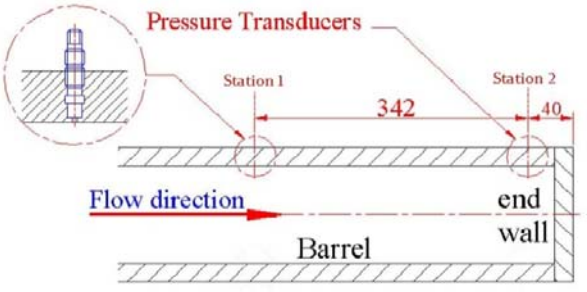

Figure-6. Pressure transducers mounted to the end of the driven section.

The shock wave speed is determined from the experimental pressure history diagram as shown in Figure-7. It is known that the distance between station 1 and station 2 is 0.342m (Figure-6), while the time required for the shock wave to travel between the two stations is obtained from the pressure history diagram at both stations. Figure- 8 shows a close up view of the incident shock wave region. For this shot for example; the shock wave speed is about 503m/s.

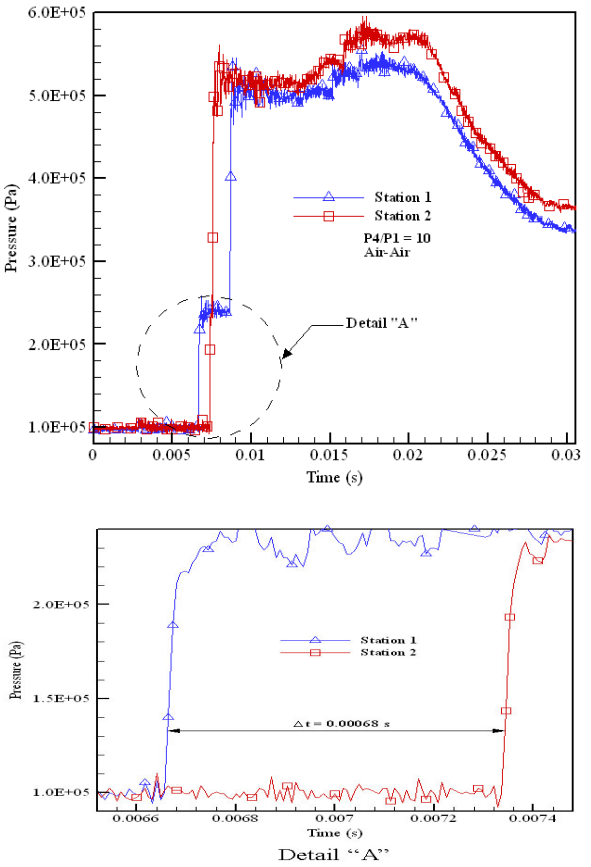

Figure-7. Experimental pressure history (P4/P1=10, Air-Air).

4. RESULTS AND DISCUSSIONS

A. Instantaneous pressure history

Numerically obtained instantaneous pressure histories for operating conditions of P4/P1=10, Air-Air with and without area contraction are shown in Figure-8. The figure helps to understand the physics of the flow inside the shock tube. When one traces the pressure history obtained with area contraction, at station 1, the first pressure jump represents the shock wave, and the second pressure jump represents the reflected shock wave. In the first jump, the pressure increases rapidly from 100 KPa to about 240 KPa. The sudden change in pressure is caused due to the arrival of the shock wave to the first pressure transducer (station 1). The shock wave travels towards the

end of the shock tube compressing the test gas, and subsequently reflects off at the closed end of the driven tube. The reflected shock wave further increases the test gas pressure to around 440 KPa, which is represented by the second jump. Following that, the reflected shock wave interacts with the contact surface. This process increases the pressure to its peak value of 540 KPa.

The same Figure also presents the instantaneous pressure history for no area contraction which is obtained at the same operating conditions (P4/P1 = 10, Air-Air). It shows similar trend as for area contraction. The shock wave increases the pressure at station 1 from 100 KPa to around 285 KPa. Following that it reflects and further increases the pressure to 670 KPa and finally interacts with the contact surface to achieve a peak pressure of 800 KPa. It is interesting to note that the pressure changes achieved with no area contraction due to the moving shock wave, reflected shock, and interaction process with the contact surface are greater than those obtained with area contraction.

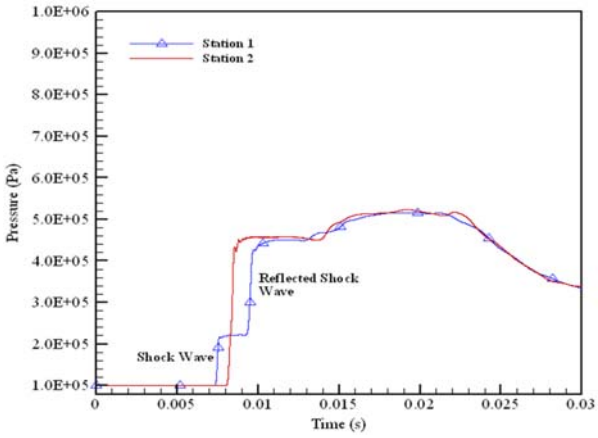

(a)

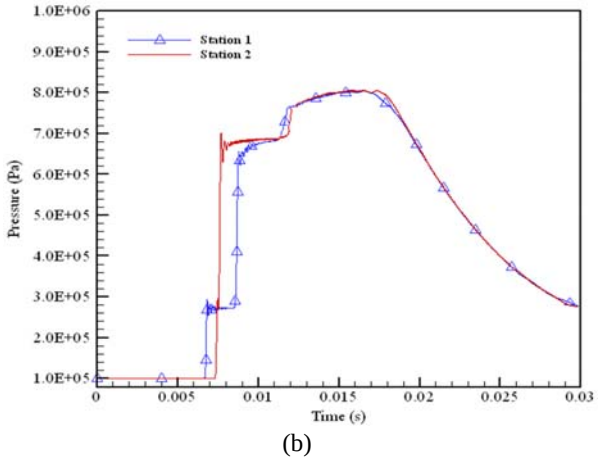

(b)

Figure-8. CFD Pressure history (a) with area contraction (b) without area contraction (P4/P1=10, Air-Air).

The same observation has been carried out when diaphragm pressure ratios (P4/P1) of 15 and 20 are used as shown in Figure-9 and Figure-10 respectively. The two figures also compare between the pressure histories obtained numerically and experimentally at station 1 and station 2.

For comparison between the CFD and the experimental pressure histories in the shock tube, both figures show that the shock wave strength and shock speed are well predicted by the CFD solver. On the other hand, over-prediction of peak pressure is observed in the CFD simulations. However, this variation is due to diaphragm rupture process which is not modelled numerically. The diaphragm is a thin sheet of aluminium used to separate the high pressure driver gas from the low pressure driven gas until it burst to initiate the flow in the experimental test facility. Experimentally, the effective area of the diaphragm opening throat after rupture was somewhat smaller than the internal area of the driven tube. This will interrupt the mass flow of the driver gas from the driver section into the driven tube, which in turn reduce the attained peak pressure.

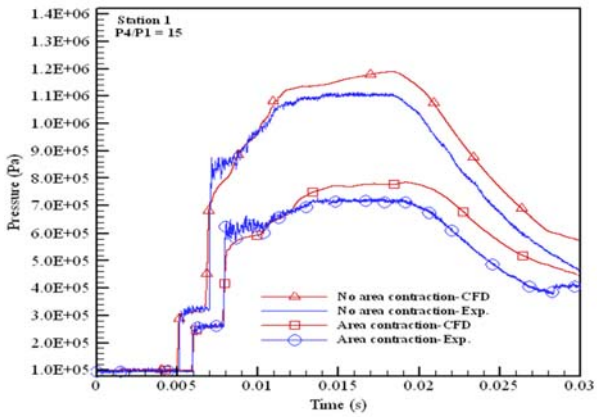

Station 1

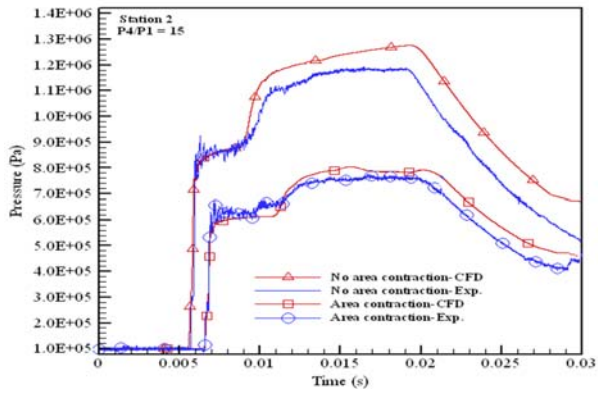

Station 2

Figure-9. Pressure history (CFD) (P4/P1=15, Air-Air).

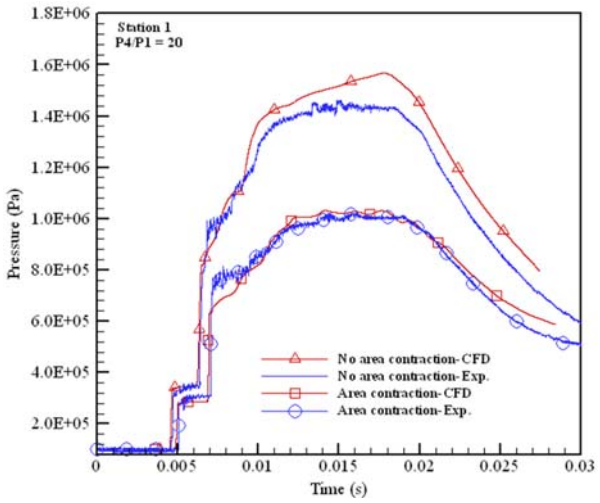

Station 1

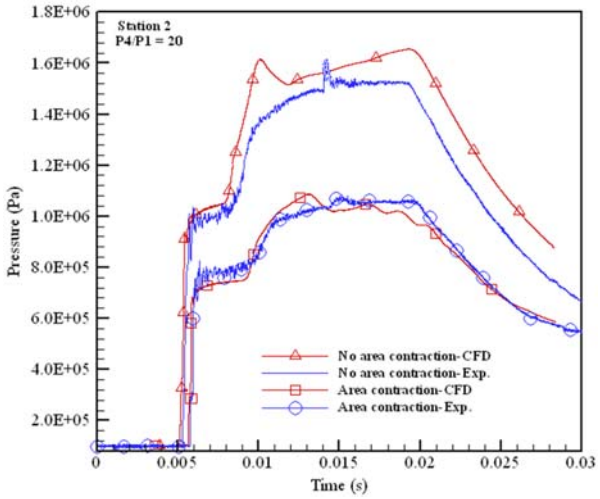

Station 2

Figure-10. Pressure history (CFD) (P4/P1=20, Air-Air).

B. x-t diagram

x-t diagram is a useful tool used to provide an overall view of flow process inside shock tube after diaphragm rupture. Figure-11 depicts the x-t diagram for density profile in the facility for shot with area contraction. From this Figure, it can be noted that after diaphragm rupture, a shock wave propagates along the driven section, followed by the contact surface. At the same time, a rarefaction waves are generated and propagate in the compression chamber. Following that, both waves reflect off at the closed ends of the shock tube. The shock wave reflects at t = 8.1ms and interacts with the contact surface at t = 11.6ms to continue its journey towards the diaphragm section. Due to the existence of area contraction in the diaphragm section, the rarefaction wave undergoes another reflection within the driver section of the facility as shown in the same Figure. The area contraction at the diaphragm section has prevented both reflected shock wave and reflected rarefaction waves from passing to the opposite sections of the facility. This process is undesirable since it is useful to examine the flow conditions at region between the reflected rarefaction wave and the contact surface for testing purposes.

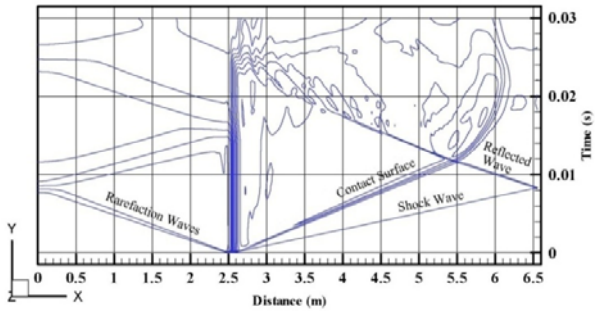

Figure-11. x-t diagram for density profile with area contraction.

The x-t diagram for density profile obtained with no area is also plotted in Figure-12. It can be seen from this diagram that the shock wave reflects at the right end of the facility at t = 7.4ms to interacts with the contact surface at t = 9.8ms. The expansion wave reflects at the closed left end of the facility and propagates from left to right until it passes to the driven section and interacts with the reflected shock wave. After the interaction process, the shock wave continues propagating in the same direction to pass the diaphragm section to the driver tube. This shows that removing the bush from the diaphragm section has allowed both reflected waves passing into the other sections of the facility and interacting with each other. From this interaction process, the total useful testing time can be determined.

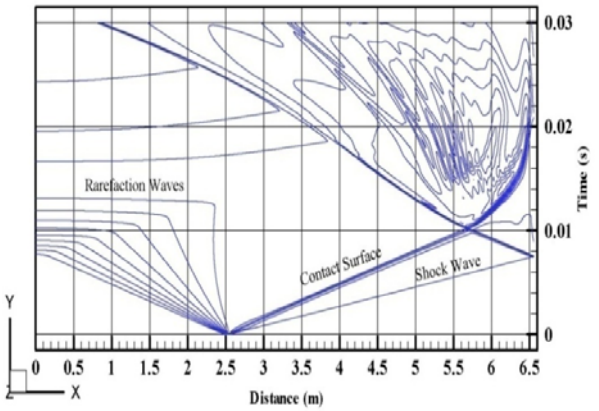

Figure-12. x-t diagram for density profile without area contraction.

C. Shock mach number

In order to summarize the area contraction effects on shock wave speed, the numerical and experimental shock wave Mach number at different operating conditions are gathered in Figure-13. Higher shock Mach numbers are obtained for shots with no area contraction as the same operating conditions are applied. For instance, shock Mach number of 1.6 is obtained for shot with area contraction at diaphragm pressure ratio (P4/P1) of 20. While at the same diaphragm pressure ratio, the shock Mach number has increased to about 1.72 when the facility was operated with no contraction. The same figure shows that the shock wave Mach number has increased by increasing the pressure ratio across the diaphragm.

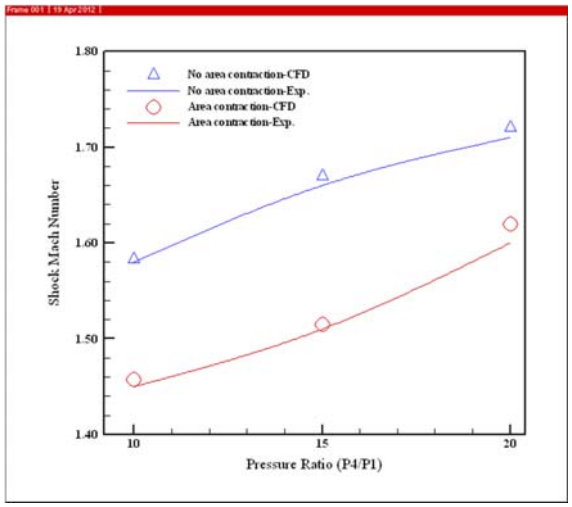

Figure-13. Shock Mach number at different operating conditions.

CONCLUSIONS

The paper described the flow process inside a short duration high speed flow shock tube. The effect of area contraction on the performance of the shock tube has been investigated numerically and experimentally. 2D-CFD solver was used to simulate the flow process in the facility. The present code showed good capability to provide the x-t diagram successfully. From this diagram the useful duration of test time can be determined. The shock strength and shock speed of the experimental and that of CFD results are very much comparable. Results also show that two-dimensional modelling of the high speed flow test facility is an effective way to obtain facility performance data. From the numerical results and experimental measurements, it has been shown that the instantaneous pressure rise and shock Mach number are significantly influenced by the presence of area contraction in the diaphragm section of the facility. The shock wave strength, peak pressure and shock Mach number have been decreased when the shock tube was operated with area contraction.

ACKNOWLEDGEMENTS

The authors would like to sincerely thank the Ministry of Higher Education (MOHE) of Malaysia for the provision of a grant with code no. FRGS/1/2013/TK01/UNITEN/01/1-20130107FRGS to support this work.

REFERENCES

Al-Falahi, A., Yusoff, M. Z., and Yusaf, T. 2008a. Development of a Short Duration Hypersonic Test Facility and Universiti Tenaga Nasional. Journal Institute of Engineers, Malaysia. 69: 32-38.

Al-Falahi, A., Yusoff, M. Z., and Yusaf, T. 2008b. Numerical simulation of inviscid transient flows in shock tube and its validations. International Conference on Fluid Mechanics, Heidelberg, Germany September 24-26.

Al-Falahi A. 2008c. Design, construction and performance evaluation of short duration high speed flow test facility. Ph.D. thesis, Univesity Tenaga Nasional, Malaysia.

Al-Falahi A., Yusoff M. Z., Shuaib N. H. and Yusaf T. 2009. Flow Instability in Shock Tube Due to Shock Wave-Boundary Layer-Contact Surface Interactions, a Numerical Study. European Journal of Scientific Research. 30: 164-176.

Briassulis G., Agui J. H., Andreopoulos J. and Watkins C. B. 1996. A shock tube research facility for high-resolution measurements for compressible turbulence. Experimental Thermal and Fluid Science. 13: 430-446.

Chue R. S. M. and Eitelberg G. 1998. Studies of the transient flows in high enthalpy shock tunnels. Experiments in fluid. 25: 474-486.

Drazin P. G. and Reid W. H. 1993. Hydrodynamic stability. Cambridge Monographs on Mechanics and Applied Mathematics, Cambridge University Press.

Goozee R. J., Jacobs P. A. and Buttsworth D. R. 2006. Simulation of a complete reflected shock tunnel showing a vortex mechanism for flow contamination. International Journal of Shock wave. 15: 165-176.

Jacob P. A. 1991. Simulation of transient flow in a shock tunnel and a high mach number nozzle. NASA Contractor Report 187606, ICASE, Report No. 91-60.

Mohsen A. M., Yusoff M. Z., Al-Falahi A. and Shuaib N. H. 2012. The effects of area contraction on shock wave strength and peak pressure in shock tube. International Journal of Automutive and Mechanical Engineering. 5: 587-596.

Satheesh K., Jagadeesh G. and Reddy K. P. J. 2007. High speed schlieren facility for visualization of flow fields in hypersonic shock tunnels. Current Science. 92: 1-2.

Wintenberger E. 2002. 6 Inch Shock Tube experiments. 315 Guggenheim, January 5.

Wilson G. J., Sharma S. P. and Gillespie W. D. 1993. Time dependent simulations of reflected shock/boundary layer interaction, AIAA Journal. 93-0480.